Article

Factors that Determine the Protein Resistance of Oligoether Self-Assembled Monolayers – Internal Hydrophilicity, Terminal Hydrophilicity, and Lateral Packing Density

Sascha Herrwerth, Wolfgang Eck, Sven Reinhardt, and Michael Grunze

J. Am. Chem. Soc., **2003**, 125 (31), 9359-9366• DOI: 10.1021/ja034820y • Publication Date (Web): 15 July 2003

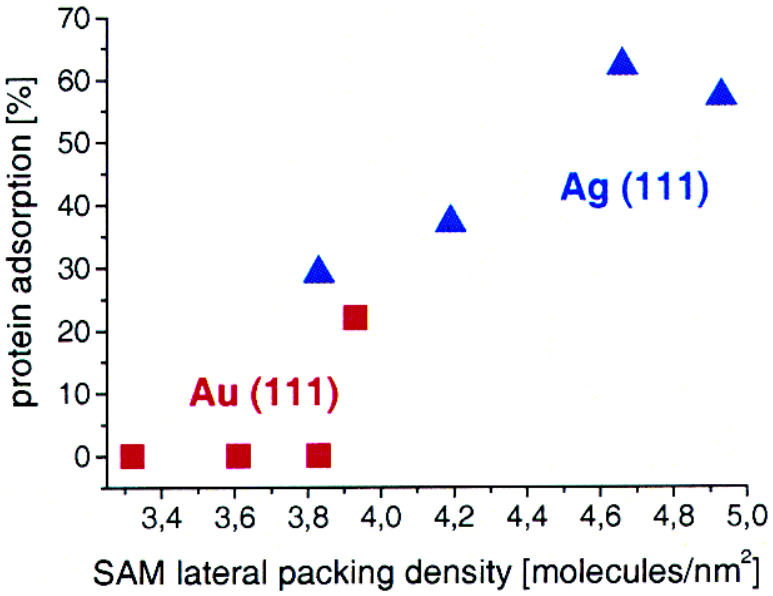

More About This Article

Additional resources and features associated with this article are available within the HTML version:

- Supporting Information
- Links to the 43 articles that cite this article, as of the time of this article download
- Access to high resolution figures
- Links to articles and content related to this article
- Copyright permission to reproduce figures and/or text from this article

View the Full Text HTML

J|A|C|S
ARTICLES
Published on Web 07/15/2003

Factors that Determine the Protein Resistance of Oligoether Self-Assembled Monolayers − Internal Hydrophilicity, Terminal Hydrophilicity, and Lateral Packing Density

Sascha Herrwerth, Wolfgang Eck,* Sven Reinhardt, and Michael Grunze*

Contribution from the Angewandte Physikalische Chemie, Universität Heidelberg, INF 253, D 69120 Heidelberg, Germany

Received February 23, 2003; E-mail: wolfgang.eck@urz.uni-heidelberg.de; michael.grunze@urz.uni-heidelberg.de

Abstract: Protein resistance of oligoether self-assembled monolayers (SAMs) on gold and silver surfaces has been investigated systematically to elucidate structural factors that determine whether a SAM will be able to resist protein adsorption. Oligo(ethylene glycol) (OEG)-, oligo(propylene glycol)-, and oligo(trimethylene glycol)-terminated alkanethiols with different chain lengths and alkyl termination were synthesized as monolayer constituents. The packing density and chemical composition of the SAMs were examined by XPS spectroscopy; the terminal hydrophilicity was characterized by contact angle measurements. IRRAS spectroscopy gave information about the chain conformation of specific monolayers; the amount of adsorbed protein as compared to alkanethiol monolayers was determined by ellipsometry. We found several factors that in combination or by themselves suppress the protein resistance of oligoether monolayers. Monolayers with a hydrophobic interior, such as those containing oligo(propylene glycol), show no protein resistance. The lateral compression of oligo(ethylene glycol) monolayers on silver generates more highly ordered monolayers and may cause decreased protein resistance, but does not necessarily lead to an all-trans chain conformation of the OEG moieties. Water contact angles higher than 70° on gold or 65° on silver reduce full protein resistance. We conclude that both internal and terminal hydrophilicity favor the protein resistance of an oligoether monolayer. It is suggested that the penetration of water molecules in the interior of the SAM is a necessary prerequisite for protein resistance. We discuss and summarize the various factors which are critical for the functionality of "inert" organic films.

Introduction

The development of surfaces that inhibit nonspecific protein adsorption has been an important subject for many medical and biotechnological applications.[1] Protein repelling surfaces are used, for example, as substrates for cell culture,[2] and as coatings for contact lenses[3] or catheters.[4] The design and preparation of surface coatings that suppress nonspecific protein adsorption with high reliability and reproducibility is of high technological interest, for example, to ensure specific recognition in biosensor applications.[5] To optimize the protein compatibility of surfaces, or to develop new and better surface coatings suitable for this purpose, a fundamental understanding of the underlying mechanisms of protein repulsion is required.

Since the early 1980s, poly(ethylene glycol) (PEG) has been used as a surface coating to prevent the adsorption of proteins and cells in buffered aqueous solution.[6] The protein resistance of high molecular weight PEG is well explained by "steric repulsion",[7] which is an entropic effect caused by the unfavorable change in free energy associated with the dehydration and confinement of polymer chains with high conformational freedom. To elucidate the underlying physical mechanisms of the protein resistance of PEG in more detail, a model system based on self-assembled monolayers of oligo(ethylene glycol) (OEG) alkanethiols on gold was introduced by Whitesides and co-workers as a molecularly defined model suitable for precise physical measurements.[8] As compared to polymeric, high molecular weight PEG, these monolayers offer the advantage of monodispersity, that is, a defined length of all chains and a defined interface to bulk water. Although the conformational freedom of the OEG end groups is restricted in these densely packed films as compared to polymeric PEG, they also show protein repellent properties. It was therefore suggested

(1) (a) *Proteins at Interfaces II, Fundamentals and Applications*; Horbett, T. A., Brash, J. L., Eds.; ACS Symposium Series; American Chemical Society: Washington, DC, 1995; Vol. 602. (b) Chuang, H. Y. K. In *Blood Compatibility*; Williams, D. F., Ed.; CRC Press: Boca Raton, FL, 1987; Vol. 1, pp 87−102.
(2) Chen, C. S.; Mrksich, M.; Huang, S.; Whitesides, G. M.; Ingber, D. E. *Science* **1997**, *276*, 1425−1428.
(3) Johnston, E.; Ratner, B. D. In *Immobilized Biomolecules in Analysis*; Cass, T., Ligler, F. S., Eds.; Oxford University Press: Oxford, U.K., 1998; pp 79−94.
(4) Stickler, D. J.; McLean, R. J. C. *Cells Mater.* **1995**, *5*, 167−182.
(5) Herrwerth, S.; Rosendahl, T.; Feng, C.; Fick, J.; Eck, W.; Himmelhaus, M.; Dahint, R.; Grunze, M. *Langmuir* **2003**, *19*, 1880−1887.
(6) (a) *Poly(ethylene Glycol) Chemistry*: *Biotechnical and Biomedical Applications*; Harris, J. M., Ed.; Plenum Press: New York, 1992. (b) Lee, J. H.; Kopecek, J.; Andrade, J. D. *J. Biomed. Mater. Res.* **1989**, *23*, 351−368. (c) Desai, N. P.; Hubbell, J. A. *Biomaterials* **1991**, *12*, 144−153.
(7) Jeon, S. I.; Lee, J. H.; Andrade, J. D.; De Gennes, P. G. *J. Colloid Interface Sci.* **1991**, *142*, 149−158.
(8) (a) Prime, K. L.; Whitesides, G. M. *Science* **1991**, *252*, 1164−1167. (b) Pale-Grosdemagne, C.; Simon, E. S.; Prime, K. L.; Whitesides, G. M. *J. Am. Chem. Soc.* **1991**, *113*, 12−20.

10.1021/ja034820y CCC: $25.00

that other mechanisms than those in the polymeric films may cause the inertness to protein adsorption in these monolayers.[9,10]

The efficiency of the protein resistance in these short and monodisperse films was shown to increase with the length of the OEG chains, with a minimum of two ethylene glycol (EG) units necessary for negligible protein adsorption under standard experimental conditions.[11] In SAMs with three EG units and methoxy termination, the protein resistant properties were found to depend on the conformation of the oligoether chains.[12] A helical conformation on gold was found to exhibit protein resistance, whereas on silver a planar all-trans conformation showed no protein repelling properties. The conformational transition between the different surfaces is caused by a higher packing density on silver that leads to lateral compression of the oligoether units.[13] A further study found that SAMs with a helical or amorphous conformation of the OEG end groups in general repel proteins.[14] More recently, different chain conformations depending on the length of the OEG units have been found by Valiokas et al.[15] for OEG-terminated alkanethiol amides on gold, but a correlation to protein resistance has not been established. In these systems, lateral compression of the OEG chains is effected by hydrogen bonds between the amide linker groups to the underlying alkanethiol which may lead to an all-trans chain conformation. An OEG-terminated alkanethiol amide with six EG units on gold exhibited a temperature-driven phase transition between a helical phase at lower temperature and phases with increasing all-trans content at higher temperatures.[16] On protein resistant polydisperse monolayers with a PEG molecular weight of 2000, a predominant helical conformation has also been found.[17]

Earlier theoretical ab initio studies on the interaction of water with OEG clusters[18] suggested that the inertness of the helical and amorphous conformers might be caused by a tightly bound interfacial layer of water that prevents direct contact between the proteins and the surface. However, Monte Carlo simulations later revealed that the interface between water and methoxy-terminated monolayers on gold with three EG units (EG_3OMe (**5**)) is characterized by a reduced water density as compared to that of bulk water[19] and that these surfaces are hydrophobic and therefore should show hydrophobic attraction.[9] The hydrophobic interaction is, however, apparently offset by electrostatic repulsion as was shown by Hähner et al.[10,20] On these monolayers on gold with three EG units (EG_3OMe (**5**)), Hähner et al. reported electrostatic repulsive forces of up to several tens of nanometers in range toward an EG_3OMe functionalized[20] and a hydrophobic AFM probe in aqueous electrolyte solution.[10] These repulsive forces are caused by an effective negative charge on the EG_3OMe and hydrophobic[21,22] surfaces, and it has been suggested[10,22] that they might be a major factor that leads to the repulsion of negatively charged proteins. The negative surface charge on these nonionic SAMs arises from the adsorption of hydroxide ions from solution, as shown in electrokinetic measurements on EG_3OMe and PEG monolayers on gold and on glass[22] and in a theoretical study based on density functional calculations.[23] The charge densities are comparable to those estimated from AFM measurements.[10] As is explained in ref 23, the negative surface charge on these nonionic monolayers originates from the adsorption of hydroxide ions which are present due to the autoionization of bulk water. Although negative surface potentials can explain the repulsive interactions between the AFM tip and the EG_3OMe films on gold substrates, we note that many other surfaces exhibit negative charges in aqueous solutions[21,22,24] which are not protein resistant. Hence, there must be other factors involved in rendering a surface "inert" in aqueous solutions which we will discuss in this paper.

Except for OEG, other functional tail groups with the ability to resist nonspecific protein adsorption have been developed for monodisperse SAMs. Prime et al. showed that a maltose-terminated SAM suppressed the adsorption of proteins.[8] Also, SAMs with tripropylenesulfoxide[25] and zwitterionic[26] tailgroups resisted the adsorption of proteins. In a general search for protein repelling SAMs, Whitesides and co-workers[27] found that hydrogen bond acceptors appear to be necessary within the SAM backbone to achieve protein repellent properties, whereas tail groups with hydrogen bond donors exhibit no protein resistance. An exception to this general rule was found in monolayers terminated with mannitol groups prepared by Mrksich and co-workers.[28] The hypothesis that the surface wettability as measured by the contact angle is a singular criterion that determines the protein resistance of a SAM has been ruled out in a recent study.[29] It was shown that oligo(ethylene glycol)-terminated surfaces show far higher protein resistance than other SAMs with different chemical termination but similar contact angles.

To broaden the understanding of the factors involved in the protein resistance of oligoether SAMs, we investigated a series of structural variations in the SAMs. We synthesized a series of oligoether-terminated alkanethiols with different oligoether backbones, different lengths, and different alkyl terminations

(9) Pertsin, A. J.; Hayashi, T.; Grunze, M. *J. Phys. Chem. B* **2002**, *106*, 12274−12281.
(10) (a) Feldman, K.; Hähner, G.; Spencer, N. D.; Harder, P.; Grunze, M. *J. Am. Chem. Soc.* **1999**, *121*, 10134−10141. (b) Dicke, C.; Hähner, G. *J. Phys. Chem. B* **2002**, *106*, 4450−4456.
(11) Prime, K. L.; Whitesides, G. M. *J. Am. Chem. Soc.* **1993**, *115*, 10714−10721.
(12) Harder, P.; Grunze, M.; Dahint, R.; Whitesides, G. M.; Laibinis, P. E. *J. Phys. Chem. B* **1998**, *102*, 426−436.
(13) Pertsin, A. J.; Grunze, M.; Garbuzova, I. A. *J. Phys. Chem. B* **1998**, *102*, 4918−4926.
(14) Harder, P.; Grunze, M.; Waite, J. H. *J. Adhes.* **2000**, *73*, 161−177.
(15) (a) Valiokas, R.; Svedhem, S.; Östblom, M.; Svensson, S. C. T.; Liedberg, B. *J. Phys. Chem. B* **2001**, *105*, 5459−5469. (b) Svedhem, S.; Hollander, C.-A.; Shi, J.; Konradsson, P.; Liedberg, B.; Svensson, S. C. T. *J. Org. Chem.* **2001**, *66*, 4494−4503.
(16) Valiokas, R.; Östblom, M.; Svedhem, S.; Svensson, S. C. T.; Liedberg, B. *J. Phys. Chem. B* **2000**, *104*, 7565−7569.
(17) Tokumitsu, S.; Liebich, A.; Herrwerth, S.; Eck, W.; Himmelhaus, M.; Grunze, M. *Langmuir* **2002**, *18*, 8862−8870.
(18) (a) Wang, R. L. C.; Kreuzer, H. J.; Grunze, M. *J. Phys. Chem. B* **1997**, *101*, 9767−9773. (b) Wang, R. L. C.; Kreuzer, H. J.; Grunze, M. *Phys. Chem. Chem. Phys.* **2000**, *2*, 3613−3622.
(19) Pertsin, A. J.; Grunze, M. *Langmuir* **2000**, *16*, 8829−8841.
(20) Dicke, C.; Feldman, K.; Eck, W.; Herrwerth, S.; Hähner, G. *Polym. Prepr.* **2000**, *41(2)*, 1444−1445.
(21) Schweiss, R.; Welzel, P.; Werner, C.; Knoll, W. *Langmuir* **2001**, *17*, 4304−4311.
(22) Chan, Y.-H. M.; Schweiss, R.; Werner, C.; Grunze, M. *Langmuir* **2003**, in press.
(23) Kreuzer, H. J.; Wang, R. L. C.; Grunze, M. *J. Am. Chem. Soc.* **2003**, *125*, 8384−8389.
(24) Zimmerman, R.; Dukhin, S.; Werner, C. *J. Phys. Chem. B* **2001**, *105*, 8544−8549.
(25) Deng, L.; Mrksich, M.; Whitesides, G. M. *J. Am. Chem. Soc.* **1996**, *118*, 5136−5137.
(26) (a) Kane, R. S.; Deschatelets, P.; Whitesides, G. M. *Langmuir* **2003**, *19*, 2388−2391. (b) Ostuni, E.; Chapman, R. G.; Liang, M. N.; Meluleni, G.; Pier, G.; Ingber, D. E.; Whitesides, G. M. *Langmuir* **2001**, *17*, 6336−6343. (c) Holmlin, R. E.; Chen, X.; Chapman, R. G.; Takayama, S.; Whitesides, G. M. *Langmuir* **2001**, *17*, 2841−2850.
(27) (a) Ostuni, E.; Chapman, R. G.; Holmlin, R. E.; Takayama, S.; Whitesides, G. M. *Langmuir* **2001**, *17*, 5605−5620. (b) Chapman, R. G.; Ostuni, E.; Takayama, S.; Holmlin, R. E.; Yan, L.; Whitesides, G. M. *J. Am. Chem. Soc.* **2000**, *122*, 8303−8304.
(28) Luk, Y.-Y.; Kato, M.; Mrksich, M. *Langmuir* **2000**, *16*, 9604−9608.
(29) Sigal, G. B.; Mrksich, M.; Whitesides, G. M. *J. Am. Chem. Soc.* **1998**, *120*, 3464−3473.

Chart 1. Overview of the Synthesized Oligoether Alkanethiols[a]

Oligo(ethylene glycol) termination 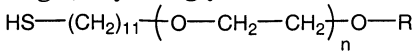 n = 1, 2, 3, 6	
EG_1OMe (**1**)	HS-$(CH_2)_{11}$-$(O\text{-}CH_2\text{-}CH_2)_1$-OMe
EG_2OH (**2**)	HS-$(CH_2)_{11}$-$(O\text{-}CH_2\text{-}CH_2)_2$-OH
EG_2OMe (**3**)	HS-$(CH_2)_{11}$-$(O\text{-}CH_2\text{-}CH_2)_2$-OMe
EG_3OH (**4**)	HS-$(CH_2)_{11}$-$(O\text{-}CH_2\text{-}CH_2)_3$-OH
EG_3OMe (**5**)	HS-$(CH_2)_{11}$-$(O\text{-}CH_2\text{-}CH_2)_3$-OMe
EG_3OEt (**6**)	HS-$(CH_2)_{11}$-$(O\text{-}CH_2\text{-}CH_2)_3$-OEt
EG_3OPr (**7**)	HS-$(CH_2)_{11}$-$(O\text{-}CH_2\text{-}CH_2)_3$-OPr
EG_3OBu (**8**)	HS-$(CH_2)_{11}$-$(O\text{-}CH_2\text{-}CH_2)_3$-OBu
EG_6OH (**9**)	HS-$(CH_2)_{11}$-$(O\text{-}CH_2\text{-}CH_2)_6$-OH
EG_6OMe (**10**)	HS-$(CH_2)_{11}$-$(O\text{-}CH_2\text{-}CH_2)_6$-OMe
EG_6OEt (**11**)	HS-$(CH_2)_{11}$-$(O\text{-}CH_2\text{-}CH_2)_6$-OEt
EG_6OPr (**12**)	HS-$(CH_2)_{11}$-$(O\text{-}CH_2\text{-}CH_2)_6$-OPr
Oligo(propylene glycol) termination 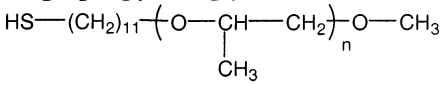 n = 2, 3, 4	
PRO_2OMe (**13**)	HS-$(CH_2)_{11}$-$(O\text{-}CH(CH_3)\text{-}CH_2)_2$-OMe
PRO_3OMe (**14**)	HS-$(CH_2)_{11}$-$(O\text{-}CH(CH_3)\text{-}CH_2)_3$-OMe
PRO_4OMe (**15**)	HS-$(CH_2)_{11}$-$(O\text{-}CH(CH_3)\text{-}CH_2)_4$-OMe
Oligo(trimethylene glycol) termination 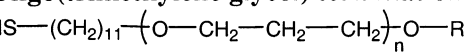 n = 3	
TRI_3OH (**16**)	HS-$(CH_2)_{11}$-$(O\text{-}CH_2\text{-}CH_2\text{-}CH_2)_3$-OH
TRI_3OMe (**17**)	HS-$(CH_2)_{11}$-$(O\text{-}CH_2\text{-}CH_2\text{-}CH_2)_3$-OMe

[a] The abbreviations used here and later in the text mean the following: EG_3OEt is a tri(ethylene glycol) unit with an ethoxy end group, PRO_3OMe is a tri(propylene glycol) unit with a methoxy end group, and TRI_3OH is a trimethylene glycol unit with OH termination. All molecules bear an undecylthiol chain on one end for anchoring on the gold and silver surfaces.

(Chart 1). The oligoether units used comprise ethylene glycol, propylene glycol, and trimethylene glycol. SAMs of these compounds were prepared on gold and on silver surfaces and were characterized by contact angle measurements, XPS, and IRRAS spectroscopy. Protein adsorption on these SAMs was examined by ellipsometric measurements using fibrinogen as a test molecule.

Results

Contact Angle Measurements. The hydroxy-terminated SAMs with oligoether end groups on gold and silver have the lowest advancing contact angles of water (32−36°, Table 1). The substrate (Au or Ag) has no specific influence on the advancing or receding contact angle.[30] Because of the higher hydrophobicity of the end group, the advancing contact angles of all methoxy-terminated monolayers are 65−76°. The lowest contact angles of the methoxy-terminated monolayers are found for the longer EG_3OMe (**5**) and EG_6OMe (**10**) chains and for TRI_3OMe (**17**) on gold and silver. The shorter OEG chains EG_1OMe (**1**) and EG_2OMe (**3**) and the oligo(propylene glycol)-terminated SAMs PRO_2OMe (**13**), PRO_3OMe (**14**), and PRO_4OMe (**15**) have slightly higher contact angles. The strong increase of the contact angles for the ethoxy-, propoxy-, and butoxy-terminated tri(ethylene glycol) and hexa(ethylene glycol) end groups reflects the rising hydrophobicity of the termination.

(30) To check for possible differences of surface reorganization in contact with water, the receding contact angles of EG_3OMe and EG_6OMe SAMs have also been measured on gold and silver. The hysteresis was constant within experimental errror, being 10−14° in all cases.

Table 1. Advancing Water Contact Angles of the SAMs on Gold and Silver

	advancing contact angle			advancing contact angle	
	Au	Ag		Au	Ag
EG_1OMe (**1**)	71°	71°	EG_6OMe (**10**)	67°	65°
EG_2OH (**2**)	33°	33°	EG_6OEt (**11**)	87°	85°
EG_2OMe (**3**)	69°	71°	EG_6OPr (**12**)	97°	96°
EG_3OH (**4**)	34°	35°	PRO_2OMe (**13**)	73°	76°
EG_3OMe (**5**)	65°	65°	PRO_3OMe (**14**)	72°	75°
EG_3OEt (**6**)	84°	84°	PRO_4OMe (**15**)	71°	73°
EG_3OPr (**7**)	94°	95°	TRI_3OH (**16**)	34°	32°
EG_3OBu (**8**)	107°	104°	TRI_3OMe (**17**)	67°	65°
EG_6OH (**9**)	32°	36°			

Table 2. Calculated and Experimental Ratios of Ether Carbon to Oxygen XPS Intensities

	C1s ether/O1s ether				C1s ether/O1s ether		
	calcd.	Au	Ag		calcd.	Au	Ag
EG_1OMe (**1**)	2/1	1.82/1	1.85/1	EG_6OMe (**10**)	2/1	2.1/1	2.1/1
EG_2OH (**2**)	1.5/1	1.51/1	1.52/1	EG_6OEt (**11**)	2/1	2.07/1	1.95/1
EG_2OMe (**3**)	2/1	1.84/1	1.87/1	EG_6OPr (**12**)	2/1	2.12/1	2.05/1
EG_3OH (**4**)	1.75/1	1.67/1	1.71/1	PRO_2OMe (**13**)	2/1	2.03/1	1.88/1
EG_3OMe (**5**)	2/1	1.87/1	1.97/1	PRO_3OMe (**14**)	2/1	1.84/1	1.85/1
EG_3OEt (**6**)	2/1	2.01/1	1.92/1	PRO_4OMe (**15**)	2/1	2.05/1	1.91/1
EG_3OPr (**7**)	2/1	2.09/1	2.11/1	TRI_3OH (**16**)	1.75/1	1.81/1	1.65/1
EG_3OBu (**8**)	2/1	1.99/1	2.05/1	TRI_3OMe (**17**)	2/1	1.89/1	1.83/1
EG_6OH (**9**)	1.86/1	1.99/1	1.83/1				

X-ray Photoelectron Spectroscopy. To ensure that the organic layers of the oligoether-terminated alkanethiols on gold and silver were free of contamination, we calculated the expected ratio of the intensities of C1s ether carbon to O1s ether oxygen signals and measured it by XP spectroscopy. Because only the oligoether units of the monolayers were considered for this purpose, the signals from both atomic species were weighted equally. For the O1s emission, a single peak at about 532.4−533 eV (depending on the monolayer and the substrate) was used to fit the data. For the C1s line, two distinct C1s peaks at about 284.4−285.1 eV for the alkyl chain and at about 286.4−287.0 eV for the ether carbon atoms were required. For all samples, the C1s/O1s ratios were close to the calculated stoichiometric ratio of ether carbon to oxygen atoms (Table 2). We therefore conclude that the monolayers were free of impurities and that the silver substrates had no significant oxygen contamination within the sensitivity limits of XPS.

The surface coverage and lateral packing density of an oligoether SAM can be determined by measurement of the attenuation of the metal substrate photoelectrons (Au 4f and Ag 3d).[12] As a reference system, unsubstituted alkanethiol SAMs ($C_{12}SH$, $C_{16}SH$, $C_{18}SH$, and $C_{20}SH$) were used to determine the attenuation of the Au and Ag substrate signals as a function of monolayer thickness (Figure 1).

In an idealized, densely packed, and defect free alkanethiol SAM with 100% coverage, the area occupied by a single chain is 21.4 Å^2 on Au(111) and 19.1 Å^2 on Ag(111).[12] This corresponds to packing densities of 4.67 molecules/nm^2 on gold or 5.24 molecules/nm^2 on silver. When the attenuation of the Au 4f and Ag 3d XPS signals by a given oligoether monolayer is compared to the attenuation by the alkanethiol reference films in Figure 1, the lateral packing density of the oligoether SAM can be calculated.

As an example, the experimental data show that the attenuation of the Au 4f substrate by an EG_3OMe (**5**) film with 18 carbon atoms and 4 oxygen atoms is identical to the attenuation by an unsubstituted C_{17} alkanethiol film on gold. This implies that an EG_3OMe monolayer has a relative coverage of 77% on gold as compared to that of an alkanethiol SAM on gold, or an average lateral packing density of 3.61 molecules/nm^2. On silver, the attenuation of the Ag 3d substrate signal by an EG_3OMe (**5**) film corresponds to the attenuation of an alkanethiol film of 17.6 carbon atoms on average. Thus, an EG_3OMe monolayer on silver has a coverage of 80% relative to an alkanethiol on silver or an average lateral packing density of 4.19 molecules/nm^2. Details of this method to evaluate packing densities have been described in ref 12.

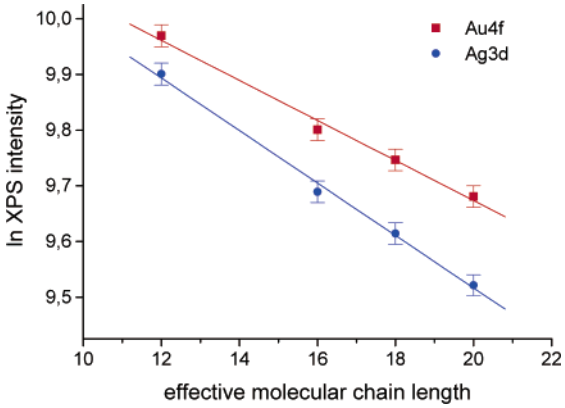

Figure 1. Attenuation of the substrate photoelectron intensity for alkanethiol SAMs with 12, 16, 18, and 20 carbon atoms and 100% surface coverage. The logarithmic Ag 3d and Au 4f intensities decrease linearly with increasing molecular chain length of the unsubstituted alkanethiols.

Table 3. Packing Density of the Oligoether-Terminated SAMs on Gold and Silver, Expressed by the Average Number of Molecules per nm^2

	molecule density [nm^{-2}]			molecule density [nm^{-2}]	
	Au	Ag		Au	Ag
EG_1OMe (**1**)	3.93	4.93	EG_6OMe (**10**)	3.32	3.83
EG_2OH (**2**)	3.93	4.66	EG_6OEt (**11**)	3.32	3.72
EG_2OMe (**3**)	3.83	4.66	EG_6OPr (**12**)	3.32	3.62
EG_3OH (**4**)	3.79	4.19	PRO_2OMe (**13**)	3.13	3.72
EG_3OMe (**5**)	3.61	4.19	PRO_3OMe (**14**)	2.99	3.56
EG_3OEt (**6**)	3.69	4.14	PRO_4OMe (**15**)	2.71	3.30
EG_3OPr (**7**)	3.79	4.19	TRI_3OH (**16**)	3.92	4.19
EG_3OBu (**8**)	3.83	4.09	TRI_3OMe (**17**)	3.60	4.40
EG_6OH (**9**)	3.46	3.62			

Table 3 shows that the oligoether-terminated alkanethiol monolayers generally have a higher packing density on silver than on gold, which correlates with the behavior of unsubstituted alkanethiols on these two substrates.

With increasing length of the OEG tail group, lower packing densities of the OEG-terminated monolayers are obtained. The monolayers of the methoxy-terminated mono(ethylene glycol) undecanethiol EG_1OMe (**1**) and the hydroxy- and methoxy-terminated di(ethylene glycol) undecanethiols EG_2OH (**2**) and EG_2OMe (**3**) have about 20% higher density on silver than on gold. For the longer EG_3- and EG_6-derivatives, the influence of the substrate becomes smaller, and the difference in packing densities between gold and silver is only 5−13%. The higher packing densities of the EG_2OMe (**3**) and EG_1OMe (**1**) monolayers, as compared to EG_6OMe (**10**) and EG_3OMe (**5**), are also reflected in the slightly higher contact angles for EG_2OMe (**3**) and EG_1OMe (**1**). Because of the shorter OEG chain, the

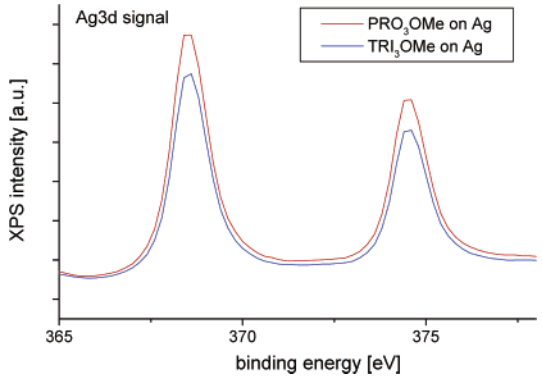

Figure 2. Ag 3d XP spectra of PRO_3OMe (**14**) and TRI_3OMe (**17**) on silver. The Ag 3d intensity of the TRI_3OMe sample is weaker due to the higher surface coverage.

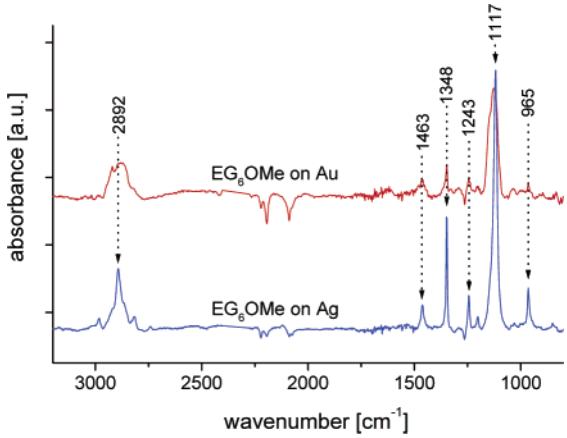

Figure 3. IRRAS spectra for EG_6OMe (**10**) monolayers on gold and silver.

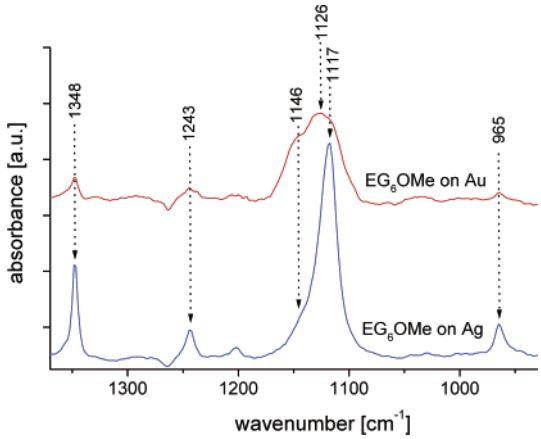

Figure 4. Fingerprint region of EG_6OMe (**10**) monolayers on gold and silver.

influence of the alkyl chain on the packing behavior is more pronounced. The alkyl termination of the OEG end group has a much weaker influence on the packing density in comparison to the chain length of the OEG end group. The densities measured here for EG_6OH (**9**) and EG_3OMe (**5**) are in good agreement with the values determined by Harder et al.[12] For EG_3OMe (**5**) on silver, we found identical results with respect to chain conformation and protein resistance, but slightly lower packing densities which might be caused by different roughness or degree of surface oxidation of the silver substrates or the use of dimethylformamide instead of ethanol as solvent for the SAM preparation.

The tri(trimethylene glycol)-terminated alkanethiol monolayers TRI_3OH (**16**) and TRI_3OMe (**17**) have packing densities approximately equal to those of the di(ethylene glycol)- and tri(ethylene glycol)-terminated SAMs. The additional methylene groups in the tri(trimethylene glycol) tail groups do not hinder effective packing of the adsorbate molecules. Correspondingly, the similar contact angles of the tri(trimethylene glycol)- and the tri(ethylene glycol)-terminated monolayers indicate comparable packing densities and order of the monolayers.

On the other hand, the oligo(propylene glycol)-terminated monolayers PRO_2OMe (**13**), PRO_3OMe (**14**), and PRO_4OMe (**15**) have lower packing densities as compared to the corresponding oligo(ethylene glycol)- or trimethylene glycol-terminated SAMs without methyl side groups. The experimental data (Figure 2) show that the attenuation of the Ag 3d substrate photoelectrons by a PRO_3OMe (**14**) film is much weaker than that of a TRI_3OMe (**17**) film with an equal number of atoms.

Obviously, the more bulky nature of the oligo(propylene glycol) groups hinders denser packing of the adsorbate molecules. The higher contact angles measured for the oligo(propylene glycol) SAMs also imply more disordered, less densely packed films and point to the significant influence of the methyl side chain.

IRRAS Experiments with EG_6OMe Monolayers on Gold and Silver. As will be shown later, we unexpectedly observed protein adsorption for EG_6OMe (**10**) monolayers on silver, a system that had not been examined previously. On the other hand, EG_6OMe (**10**) monolayers on gold are fully resistant to protein adsorption, which is consistent with earlier results.[11] The EG_6OMe (**10**) monolayers on gold and silver vary in their relative surface coverage (see Table 3) but show nearly no difference in their advancing water contact angles (see Table 1). Therefore, we characterized the monolayers of EG_6OMe (**10**) on gold and silver in more detail by IR spectroscopy to analyze possible differences in their molecular order and conformation.

The IR spectra of EG_6OMe (**10**) on gold and silver (Figure 3) reveal structural differences that strongly depend on the substrate. The EG_6OMe (**10**) spectrum on silver shows very strong characteristic peaks at 965 cm^{-1} (CH_2 rocking mode), 1117 cm^{-1} (COC stretching mode), 1243 cm^{-1} (CH_2 twisting mode), 1348 cm^{-1} (CH_2 wagging mode), and 1463 cm^{-1} (CH_2 scissoring mode) in the fingerprint region and at 2892 cm^{-1} (CH_2 stretching mode) in the CH stretching region. On gold, the spectral intensities of the peaks in the fingerprint region are much weaker, and the COC stretching mode at 1117 cm^{-1} is broader than on silver. The band at 2892 cm^{-1} does not dominate in the CH stretching region of EG_6OMe (**10**) on gold as it does on silver. Rather, a broad signal is observed in the CH region on gold.

The detailed spectrum of the fingerprint region (Figure 4) of EG_6OMe (**10**) on silver shows a characteristic, very strong skeletal peak at 1117 cm^{-1} with a weak shoulder appearing on the high-frequency side at 1146 cm^{-1}. The intensities and features of the peaks at 1463, 1348, 1243, and 965 cm^{-1}, respectively, as well as the strong and sharp skeletal peak at 1117 cm^{-1}, indicate the presence of a highly oriented and crystalline helical OEG phase which does, however, show protein adsorption as described later. On gold, the COC stretching band has a different shape and is shifted to higher frequencies than that on silver. The detailed spectrum shows a

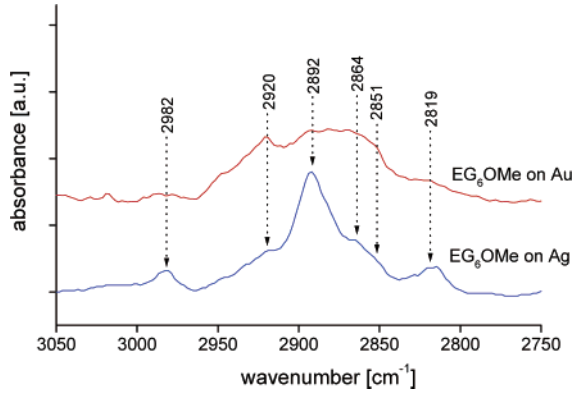

Figure 5. CH stretching region of EG_6OMe (**10**) monolayers on gold and silver.

broad peak around 1126 cm^{-1} that can be separated into at least three signals at 1146, 1126, and 1117 cm^{-1}. This and the significant decrease of the intensity of the signals at 1463, 1348, 1243, and 965 cm^{-1} indicate that the OEG chains on gold are less oriented and in a more amorphous conformation which was found to be protein resistant. On silver, the presence of a highly ordered and crystalline helical OEG phase with a higher packing density and less defects than on gold leads to loss of protein resistance of the monolayers, revealing that − contrary to previous suggestions − the molecular conformation in the SAM per se is not a sufficient indicator for protein resistance.

The detailed spectra of the CH stretching bands show quite similar differences (Figure 5). The EG_6OMe (**10**) monolayer on silver shows a very strong CH stretching peak at 2892 cm^{-1} characteristic for the crystalline helical conformation of the OEG phase.[12,16] On gold, a different shape of the peak together with a strong decrease in intensity is observed. Instead, a broad band appears from 2840 to 2960 cm^{-1}, which implies an amorphous and less oriented conformation of the OEG groups on gold.

Protein Adsorption Experiments. Fibrinogen adsorption on the different oligoether-terminated SAMs was quantified relative to protein adsorption on reference monolayers of hexadecane thiol on the respective substrates. An ex-situ ellipsometric technique similar to the one developed by Whitesides and co-workers[8,11] was used to determine the relative thickness of adsorbed protein layers that remain on the SAMs after rinsing with water (see experimental section in the Supporting Information). The detection limit of this technique is a few percents of a monolayer, and it is less sensitive than in-situ ellipsometry or surface plasmon resonance. However, it gives well reproducible information on the relative amount of protein that is irreversibly adsorbed on different surfaces and cannot be removed by rinsing.

The data shown in Table 4 and Figures 6 and 7 indicate that all hydroxy-terminated SAMs with oligo(ethylene glycol) or tri(trimethylene glycol) tail groups show no protein adsorption on gold and silver. However, the methoxy-terminated SAMs with OEG tail groups (EG_2OMe (**3**), EG_3OMe (**5**), and EG_6OMe (**10**)) are only protein resistant on gold. On silver, where higher packing densities are observed, the methoxy-terminated SAMs are no longer protein resistant. The monolayers of EG_1OMe (**1**) adsorb proteins both on gold and on silver, which is fully consistent with the previous result that at least two ethylene glycol groups are necessary for protein resistance.[11] The methoxy-terminated SAMs with tri(trimethylene glycol) tail groups (TRI_3OMe (**17**)) show behavior similar

Table 4. Amount of Adsorbed Fibrinogen on SAMs on Gold and Silver, Measured by the Ellipsometric Thickness of the Protein Layer and Normalized to the Amount of Fibrinogen Adsorbed on a Monolayer of Hexadecanethiol ($C_{16}SH$) on Gold (=100%)

	protein adsorption [%]			protein adsorption [%]	
	Au	Ag		Au	Ag
EG_1OMe (**1**)	22	57	EG_6OMe (**10**)	0	35
EG_2OH (**2**)	0	0	EG_6OEt (**11**)	51	89
EG_2OMe (**3**)	0	62	EG_6OPr (**12**)	69	100
EG_3OH (**4**)	0	0	PRO_2OMe (**13**)	52	87
EG_3OMe (**5**)	0	37	PRO_3OMe (**14**)	49	80
EG_3OEt (**6**)	60	88	PRO_4OMe (**15**)	42	60
EG_3OPr (**7**)	79	93	TRI_3OH (**16**)	0	0
EG_3OBu (**8**)	77	98	TRI_3OMe (**17**)	0	52
EG_6OH (**9**)	0	0			

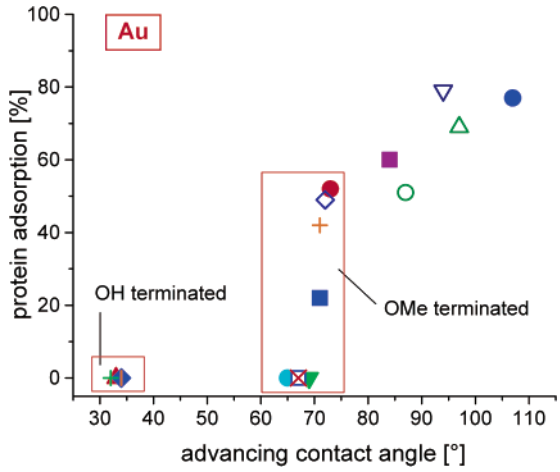

Figure 6. Amount of protein adsorption on a given oligoether SAM on gold normalized to the amount of protein adsorbed on a monolayer of hexadecanethiol on gold (100%) versus advancing aqueous contact angle of the SAM. Symbols: red ▲, EG_2OH; orange |, EG_3OH; green +, EG_6OH; blue ◆, TRI_3OH; blue ■, EG_1OMe; green ▼, EG_2OMe; light blue ●, EG_3OMe; red ×, EG_6OMe; blue □, TRI_3OMe; red ●, PRO_2OMe; blue ◇, PRO_3OMe; orange +, PRO_4OMe; purple ■, EG_3OEt; green ○, EG_6OEt; blue ▽, EG_3OPr; green △, EG_6OPr; blue ●, EG_3OBu.

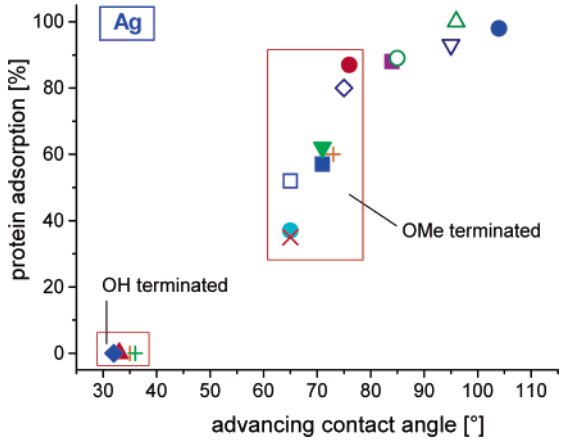

Figure 7. Amount of protein adsorption on a given oligoether SAM on silver normalized to the amount of protein adsorbed on a monolayer of hexadecanethiol on gold (100%) versus advancing aqueous contact angle of the SAM. Symbols are identical to those in Figure 6.

to that of the EG_3OMe and EG_6OMe monolayers: on gold, they are protein resistant, but on silver, they show even stronger adsorption. In remarkable contrast, all SAMs with oligo(propylene glycol) tail groups adsorb proteins on gold and silver. These

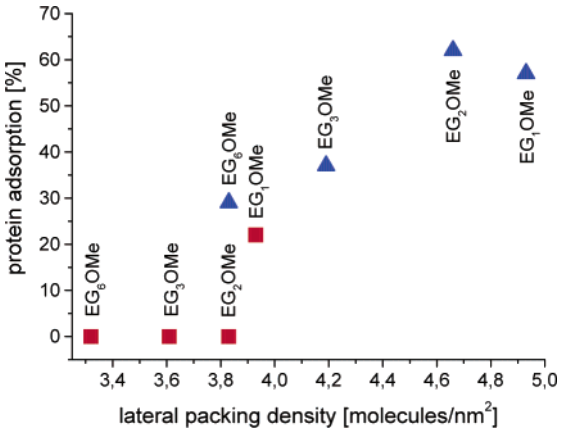

Figure 8. Amount of protein adsorption versus lateral packing densities of the methoxy-terminated SAMs with oligo(ethylene glycol) tail groups on gold and silver. Red squares are monolayers on gold, and blue triangles are monolayers on silver.

data show that the character of the oligoether tail group influences the protein resistance of the SAMs. Only the SAMs with a hydrophilic interior show protein resistance under the conditions used in our study. It is well known that high molecular weight poly(propylene glycol) is a water-insoluble polymer, whereas both poly(ethylene glycol) and poly(trimethylene glycol) are water-soluble.[31] By analogy, both for oligo(ethylene glcyol) alkyl ethers[32] and for poly(trimethylene glycol),[33] hydrates have been reported, but not for polypropylene glycol.

The SAMs with oligo(ethylene glycol) tail groups and the longer ethoxy, propoxy, or butoxy termination show strong protein adsorption due to their more hydrophobic surface properties. This indicates that besides the inner hydrophilicity also the terminal hydrophilicity or wettability is an important factor for protein adsorption. On gold, the oligoether-terminated monolayers do not show any significant protein adsorption at advancing contact angles below 70° (Figure 6). For higher contact angles, an increase of protein adsorption is observed. On silver (Figure 7), protein adsorption can be detected for slightly lower contact angles as compared to the films on gold. For the methoxy-terminated monolayers on gold and on silver, there is a high variability in protein adsorption that depends on the length and type of the oligoether chain.

In Figure 8, we show that protein adsorption on the methoxy-terminated SAMs with oligo(ethylene glycol) tail groups is a function of the lateral packing density, with a transition from nonadsorbing to adsorbing above packing densities of about 3.85 molecules/nm^2. The packing density in turn depends on the length of the oligo(ethylene glycol) chain. In contrast to the methoxy-terminated OEG SAMs, the hydroxy-terminated OEG SAMs show full protein resistance also for short chain lengths and high packing densities on silver (Table 4; Figures 6, 7). Because, in terms of surface wettability, the methoxy-terminated SAMs are at the borderline of protein resistance, suitable packing characteristics of their oligoether units are of higher significance than for hydroxy-terminated monolayers.

That EG$_6$OMe (**10**) monolayers on gold are resistant to protein adsorption is fully consistent with previous results.[11] Earlier experiments by Harder et al.[12] have shown that, in the special case of EG$_3$OMe (**5**) SAMs, the protein resistance is coupled to the molecular conformation of the OEG groups. This conclusion can, however, not be generalized, because on silver densely packed EG$_3$OMe (**5**) monolayers with an all-trans conformation and EG$_6$OMe (**10**) SAMs with a highly ordered crystalline helical structure both adsorb proteins.

The dependence of protein adsorption on lateral density is a new and important aspect. It revises our previous model that protein resistance is determined by molecular conformation; rather, lateral density (which, however, determines molecular conformation) seems to be the important variable.

Discussion

Our results show that several factors are required to make an oligoether SAM protein resistant. First, an interior hydrophilic chemical structure is necessary, because only the oligo(ethylene glycol) and oligo(trimethylene glycol) SAMs exhibit protein resistance, but no repelling properties are found on the hydrophobic oligo(propylene glycol) SAMs. Quite similarly, the lateral compression of a methoxy-terminated hexa(ethylene glycol) SAM on silver leads to reduced protein resistance, although a helical conformation is retained, and the SAM is highly ordered. This is in excellent agreement with a recent report by Vanderah et al.[34] based on IRRAS data, who found that a methoxy-terminated hexa(ethylene glycol) SAM on gold without an alkyl spacer chain showed reduced protein resistance when a highly ordered crystalline helical conformation was present. Only when disorder and a larger number of defects were introduced into the film by assembly from solvents other than ethanol was full protein resistance obtained.

These results imply that either a relaxed lateral packing density as found in SAMs on gold surfaces or some disorder or defects of the monolayer are necessary for high protein resistance. For the methoxy-terminated monolayers, packing densities exceeding a well-defined threshold value (see Figure 8) lead to a loss of resistance; for example, EG$_3$OMe-terminated monolayers with a highly ordered all-trans conformation on silver show protein adsorption.[12] Similarly, SAMs of 11-mercaptoundecan-1-ol on gold with a highly hydrophilic surface and contact angles below 15° are not resistant to fibrinogen adsorption,[29] because no hydrophilic interior is present. We conclude from our experiments that water must be able to penetrate into the SAM to achieve resistance to protein adsorption. That water penetration and lateral density are correlated has been shown in grand canonical Monte Carlo simulations (GCMC).[9,19] The fact that the protein resistance increases with higher chain length of the OEG units[11] also suggests that a higher water content in the SAM leads to better protein repulsion. In a very recent study, Vanderah et al. have shown by electrochemical impedance spectroscopy that oligo(ethylene glycol)-terminated SAMs on gold contain water when they are disordered and protein resistant, but that water penetration into a non-protein resistant and highly ordered oligo(ethylene glycol) SAM is slow.[35]

The terminal hydrophobicity of the films plays an equally important role. As a general rule, longer alkyl termini and higher

(31) (a) Gagnon, S. D. *Encycl. Polym. Sci. Eng.* **1986**, *6*, 273−307. (b) Dreyfuss, M. P.; Dreyfuss, P. *Encycl. Polym. Sci. Eng.* **1987**, *10*, 653−670.
(32) Heusch, R. *Ber. Bunsen-Ges.* **1979**, *83*, 834−840.
(33) Yoshida, S.; Sakiyama, M.; Seki, S. *Polym. J. (Tokyo)* **1970**, *1*, 573−581.
(34) Vanderah, D. J.; Valincius, G.; Meuse, C. W. *Langmuir* **2002**, *18*, 4674−4680.
(35) Vanderah, D. J.; Arsenault, J.; La, H.; Gates, R. S.; Silin, V.; Meuse, C. W. *Langmuir* **2003**, *19*, 3752−3756.

terminal hydrophobicity lead to reduced protein repelling properties. Contact angles up to 70° on gold and 65° on silver seem to be tolerable for full protein resistance. Hydroxy termination and therefore the highest hydrophilicity of the monolayer generate in all cases the highest protein resistance. This is in excellent agreement with recent results by Vogler[36] who reported that long-range attractive forces are found only between hydrophobic surfaces exhibiting a water contact angle $> 65°$, but short-range repulsive forces are detected between hydrophilic surfaces with contact angles below this value. The reason for the general observation that a balance of forces is achieved at a contact angle of about 65° has been discussed and explained by us in a previous publication.[37]

Our results indicate that only the combination of several key factors, the hydrophilicity of the termination, the hydrophilicity of the internal units, and the lateral packing density, allows the formation of a SAM that is fully protein resistant. If the ability of a polyether SAM to coordinate water both in its interior and on its surface is reduced when one of these factors is unfavorable or absent, the overall protein resistance decreases.

As was shown in two other recent studies,[22,23] the negative surface charge inferred from the surface force experiments on EG_3OMe SAMs is due to preferential adsorption of hydroxide ions from solution. Adsorption involves hydrogen bonding between the hydroxide ion and the terminal hydrogen atoms in the SAM surface, where it seems to be of less importance[23] if the terminal function is a methoxy or hydroxy moiety. This is supported by experiments which show that negative surface charging in aqueous solution is by no means unique to the EG_3OMe SAMs, but occurs to about the same extent (limited apparently by the repulsive electrostatic interaction between the adsorbed ions) on hexadecanethiolate and 11-mercaptoundecan-1-ol SAMs on gold,[22] which are clearly not protein resistant and are not penetrated by water. As was discussed by Kreuzer et al. in ref 23, one important role of water inside the SAM is the formation of an additional hydrogen bond to the hydroxide ion on the surface, and thereby the stabilization of the adsorbed ion in absolute terms, but also against lateral displacement. Hypothetically, protons or hydronium ions solvated within defect sites of the oligoether monolayer could lead to further immobilization of the adsorbed negative charge layer. Hence, when the hydroxide ions are stabilized against displacement, an approaching negatively charged object cannot replace the negative surface charge and therefore will not adsorb on the surface. Adsorption of cationic polyelectrolytes onto EG_3OH surfaces was shown to depend on the pH of the solution,[38] presumably due to changes in the charge density and sign both on the macromolecule and on the SAM surface.

Only at high ion concentration or low pH[10b,39] is the negative surface charge screened or neutralized, respectively, and other forces and effects dominate the adsorption behavior at a distance of ≤ 10 nm in front of the surface. Typically, an attractive interaction is observed, in agreement with the hydrophobic nature of perfect (theoretical) SAMs as was revealed in the GCMC simulations for the EG_3OMe SAMs both on Au and on Ag substrates in contact with water.[9] However, real surfaces may have a less than ideal packing density and hence different hydration properties that lead to repulsive solvation forces at close approach,[37] in the extreme for long chain and polydisperse oligoethers leading to a mechanism in which resistance to dehydration similar to polymeric PEG determines the adsorption behavior.

Conclusions

In this paper, we have studied the importance of internal and external hydrophilicity of oligoether SAMs for protein resistance. We conclude that only the combination of several factors, the hydrophilicity of the termination, the hydrophilicity of the internal units, and the lateral packing density, allows the formation of a SAM which is fully protein resistant. If the ability of a polyether SAM to coordinate water both in its interior and on its surface is reduced when one of these factors is unfavorable or absent, the overall protein resistance decreases.

Acknowledgment. We thank Roman Glass and Alexander Küller for help with the synthesis of several compounds and Sabina Tatur for help with contact angle measurements. This work was supported by the Deutsche Forschungsgemeinschaft, the Office of Naval Research, and the Fonds der Chemischen Industrie.

Supporting Information Available: Experimental section (PDF). This material is available free of charge via the Internet at http://pubs.acs.org.

JA034820Y

(36) (a) Vogler, E. A. *J. Biomater. Sci., Polym. Ed.* **1999**, *10*, 1015−1045. (b) Vogler, E. A. *Adv. Colloid Interface Sci.* **1998**, *74*, 69−117.
(37) Hayashi, T.; Pertsin, A. J.; Grunze, M. *J. Chem. Phys.* **2002**, *117*, 6271−6280.
(38) (a) Clark, S. L.; Hammond, P. T. *Langmuir* **2000**, *16*, 10206−10214. (b) Jiang, X.-P.; Clark, S. L.; Hammond, P. T. *Adv. Mater.* **2001**, *13*, 1669−1673. (c) Jiang, X.; Ortiz, C.; Hammond, P. T. *Langmuir* **2002**, *18*, 1131−1143.
(39) Dicke, C.; Hähner, G. *J. Am. Chem. Soc.* **2002**, *124*, 12619−12625.